Proceedings World Geothermal Congress 2020+1
Reykjavik, Iceland, April - October 2021

Reactive Transport model of CO_2 and H_2S mineral Sequestration at the CarbFix2 Reinjection Site, Hellisheiði Geothermal Power Plant, SW-Iceland

Thomas M.P. Ratouis, Sandra O. Snæbjörnsdóttir, Bergur Sigfússon, Ingvi Gunnarsson, Martin J. Voigt, and Edda S. Aradóttir

Reykjavik Energy, Bæjarháls 9, 110 Reykjavík, Iceland

Thomas.Ratouis@or.is

Keywords: Modelling, reactive transport, geochemistry, carbon sequestration, geothermal engineering, climate change

ABSTRACT

Non-condensable gases are being injected at the Husmuli reinjection site of the Hellisheiði Geothermal Power Plant in Iceland using the CarbFix method to dispose and permanently store CO_2 and H_2S by underground mineral storage. At current rate, about 10,000 tonnes of CO_2 are injected annually along with about 5,000 tonnes of H_2S. The injection of CO_2 and H_2 takes place in the Húsmúli reinjection area and has been an integral part of the operations at the Hellisheiði Geothermal Power Plant since 2014.

Coupled modelling of fluid flow and reactive transport using the TOUGH2/iTOUGH2 and TOUGHREACT simulators is being developed to study the injection of dissolved CO_2 and H_2S in basaltic rocks. The model aims to evaluate the dynamic fluid-rock interactions to identify mineralization processes under reservoir conditions. The target reservoir is an altered fractured olivine tholeiitic lava extending from the Husmuli reinjection site to the Skardsmýrarfjall production zone at depths ranging from -700 to -2000 masl.

One-dimensional reactive transport models of the CarbFix injection of a CO_2-H_2S fluid mixture in the fractured reservoir between the CarbFix reinjection site to the Skardsmýrarfjall production zone are developed. The models were set at an elevation comprised between -700 and -1800 masl where reservoir temperatures range from 220 to 260 °C. The CarbFix injection is modelled by integrating a simple wellbore mixing model with one-dimensional reservoir models at the depth at which the CarbFix fluid enters the host rock. The wellbore model simulation the mixing of the separated water and the gas-charged condensate and the resulting fluid is used as the initial chemistry for the fluid injected in the reservoir models. The average chemistry of the background reservoir chemistry as well as the primary and secondary minerals present in the basaltic reservoir were included in the model as the basis for the reactive chemistry. The simulations use the updated thermodynamic databases for mineral carbonation compiled at the University of Iceland as part of the CarbFix2 project. The simulation results showed successful mineral sequestration of CO_2 and H_2S under reservoir condition at the CarbFix site. CO_2 will mainly be mineralized into calcite and to a lesser extent ankerite and H_2S into pyrite. The results also show competition mechanism in form of clays and epidote precipitation.

1. INTRODUCTION

Reducing anthropogenic CO_2 in the atmosphere is among the great challenges of this century (Broecker, 2007). Large scale capture and sequestration of atmospheric CO_2 (CCS) is a key in the transition to a low-carbon future and holds a large role in the global response to climate change (IEA, 2016). In situ mineral sequestration is among the suggested methods (Metz *et al.* 2005; Schrag, 2007). The technology developed by the CarbFix project is an integrated process of carbon capture and mineral sequestration (Aradóttir *et al.*, 2020). It consists of soluble gas mixture capture in water followed by the direct injection of the resulting CO_2-H_2S-charged water into basaltic rock, where much of the dissolved carbon and sulfur are mineralized within months (Matter *et al.* 2016, Gunnarsson *et al.* 2018). In in situ mineral carbonation, the injected CO_2 and H_2S combine with dissolved metals to form carbonate minerals, such as calcite ($CaCO_3$), magnesite ($MgCO_3$), Ankerite ($CaFe(CO_3)_2$), or siderite ($FeCO_3$) and sulfur bearing minerals, such as pyrite ($FeSO_4$) that are stable and environmentally benign over geological time scales. Formation of these minerals enhances the stability of injected CO_2 substantially (Metz *et al.* 2005; Oelkers *et al.* 2008). This method provides a safe, long-term storage of carbon dioxide and other acid gases and may be applied for CCS projects at other sites.

Geochemical modelling is widely used to quantify chemical reactions occurring between fluids and solid phases over a wide range of temperature and pressures. Carbon storage in basalt rely on complex CO_2/H_2S-water-basalt interactions to make divalent cations available and fix CO_2 and H_2S as stable minerals. Reactive transport models combine mass transport and equilibrium speciation of multi-component systems and provide an integrated way to look at the complex interplay of material flow, transport and reactions that characterizes subsurface processes (Steefel *et al.* 2005). Reactive transport models are therefore ideal to simulate the injection of an acidic solution of dissolved CO_2/H_2S in basalt in the subsurface and resulting geochemical reactions and flow processes.

Numerical reactive transport simulations are used to evaluate the fluid rock interaction, formation and dissolution of minerals and their spatial and temporal occurrences in the reservoir. Reactive transport models also provide tools to quantify the amount of CO_2 that can be mineralized and to predict and optimize long-term management of injection sites. In this work, we present the modelling approach and the development of one-dimensional reactive transport models of the gas enriched mixture into the CarbFix reservoir and the mineral alteration associated with injecting dissolved CO_2 and H_2S into basalts. The TOUGHREACT suite of codes (Xu *et al.* 2006, Sonnenthal *et al.* 2018) developed at Lawrence Berkeley National Laboratory, California, allow the full coupling of thermal, hydrological, and chemical processes and were used for the reactive transport simulations of the CarbFix injection.

2. THE CARBFIX SITE

2.1 Site description

The Hellisheiði field is located at the southern part of the Hengill volcanic system, which was formed by several volcanic cycles during spreading episodes in the rift zone. The Hengill central volcano occupies the central part of a 60–100 km long and 3–5 km wide volcanic NESW trending fissure swarm with a graben structure. The Hellisheiði geothermal field is characterized by high heat flow and extensive geothermal activity associated with shallow level crustal magma chambers or dyke swarms. The Hellisheiði Power plant is a combined thermal energy and electricity power plant consisting of six 45 MWe high pressure and one 33 MWe low pressure turbine generator units and a 133 MWth thermal energy production unit. 61 production wells and 17 reinjection wells have been drilled in the Hellisheiði geothermal field to provide steam for the power generation, and for separated water disposal. The CarbFix2 site is located at the Húsmúli reinjection site in the northern part of the Hellisheiði field (Figure 1), at the western side of the graben structure, with large normal faults having a total throw of more than 300m (Franzson *et al.* 2010,). These faults contribute significantly to the permeability in the area (Kristjánsson *et al.* 2016, Ratouis *et al.* 2019).

Injection of CO_2 and H_2Sas part of the CarbFix2 project has been an integral part of the operations at the Hellisheiði Geothermal Power Plant in SW-Iceland since 2014. At current rate, about 10,000 tonnes of CO_2 are injected annually along with about 5,000 tonnes of H_2S are injected into HN-16 reinjection well (Sigfússon *et al.* 2018). Four production wells located within 2 km down gradient from the injection well are regularly sampled to monitor the impact of the gas-enriched mixture injection at the CarbFix reinjection site (Figure 1). The HN-16 CarbFix2 injection well, as well as the HE-31, HE-48, HE-44, and HE-33 monitoring wells used in this study are directionally drilled to depths of -1625, -1715, -1319, - 1762, and -813 masl respectively, such that they intersect high permeability fractures at depths below 800 m (Snæbjörnsdóttir *et al.* 2018). The maximum down-hole temperature in the production wells ranges from ~260-285 °C. The well paths are shown in Figure 1. The wells are cased off down to an elevation comprised between -134 and -343 masl.

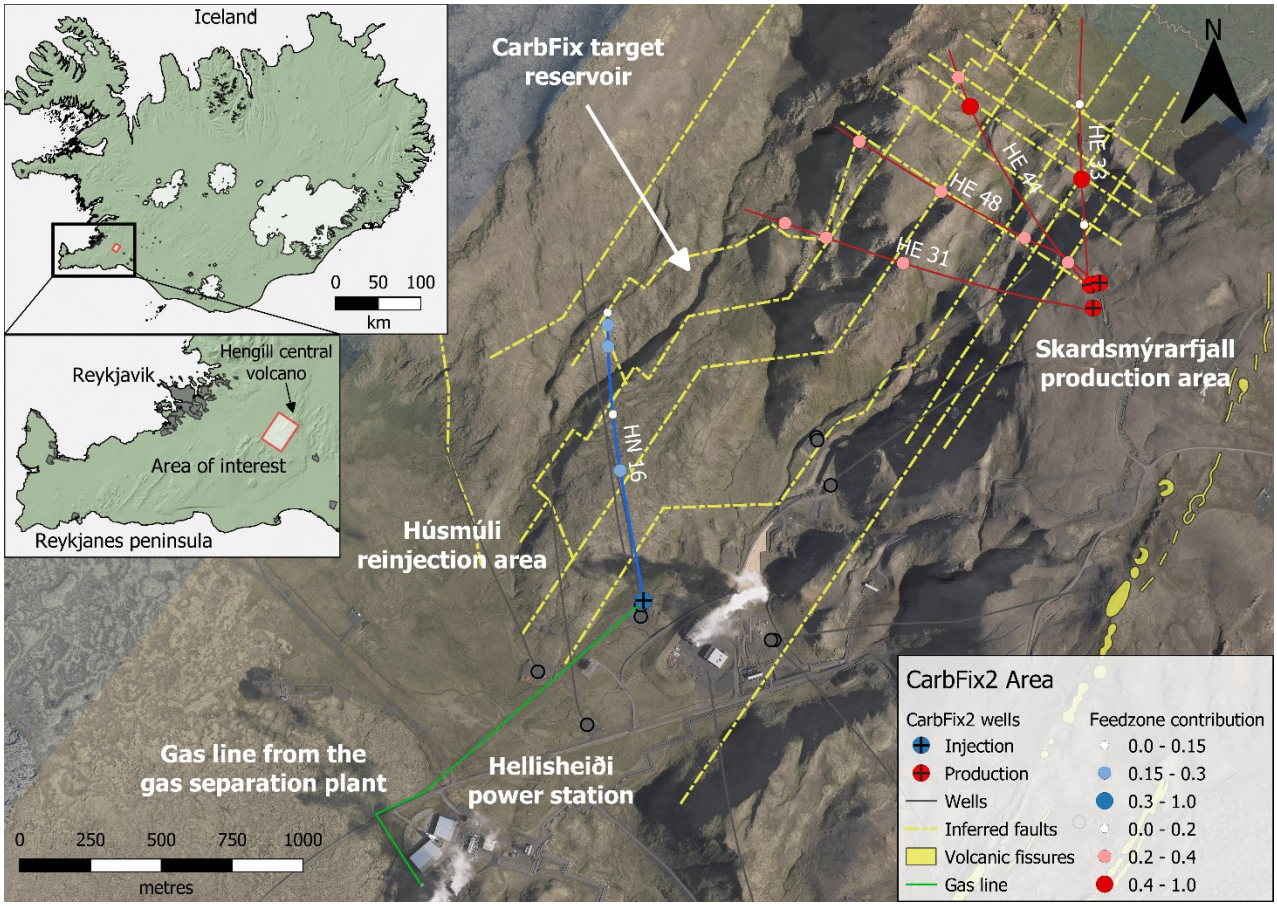

Figure 1: Overview of the CarbFix2 injection site. The gas charged water pipe (shown in green) connects the separation plant to the injection well. Injection was into well HN-16 (shown in blue). The four monitoring wells (HE-31, HE-48, HE-44, and HE-33 each shown in red) are located within 2 km down gradient from the injection well. Intersected faults are shown in yellow and feedzones location and contribution are represent by blue or red circles. The three feedzones which contributes the most the injection are labelled Feedzones 1,2, and 3.

2.1 Geological setting of the CarbFix reservoir

The subsurface at the CarbFix2 injection site consist of altered olivine tholeiitic basalts (Snæbjörnsdóttir *et al.* 2018). Below the well's casing depth hyaloclastic formations dominate the stratigraphy. These formations are very heterogeneous, ranging from crystalline pillow basalts to almost pure volcanic glass (Snæbjörnsdóttir *et al.* 2018). Below -1300 masl depth highly altered crystalline rocks intersected by intrusions are found (Snæbjörnsdóttir *et al.* 2018). This formation is the "base" of the Hengill volcano,

formed prior to the onset of central volcanic activity in the Hengill area. These two units constitute the geothermal reservoir of the Hellisheiði field and the target CarbFix reservoir.

In geothermal environments such as the Hellisheiði field, primary minerals usually tend to alter to secondary minerals that are more stable at the high temperatures encountered within a geothermal system. The formation of these alteration minerals is usually dependent on the temperature, permeability, pressure, fluid composition, initial composition of the rock and the duration of the hydrothermal activity (Lagat, 2009). As the hydrothermal fluid flows through the rock it alters the composition of the rocks by adding or removing or redistributing components. Studies of geothermal alteration of basaltic rocks in Iceland show sequences of alteration mineral assemblages that change with increased depth and temperature; these are identified as zones of alteration as described below, reflecting the dominant temperature of the system when the minerals were formed (Snæbjörnsdóttir *et al.* 2018). The first sign of hydrothermal alteration is the formation of smectites and zeolites (Figure 2). Quartz starts forming at about >180 °C, and smectites become interlayered with chlorite, forming mixed layer clays at temperatures around >200 °C (Figure 2). The high temperature hydrothermal alteration is characterized by the formation of chlorite and epidote above 230-250 °C (Figure 2). Epidote becomes more abundant along with prehnite and actinolite at temperatures above 280 °C (Figure 2).

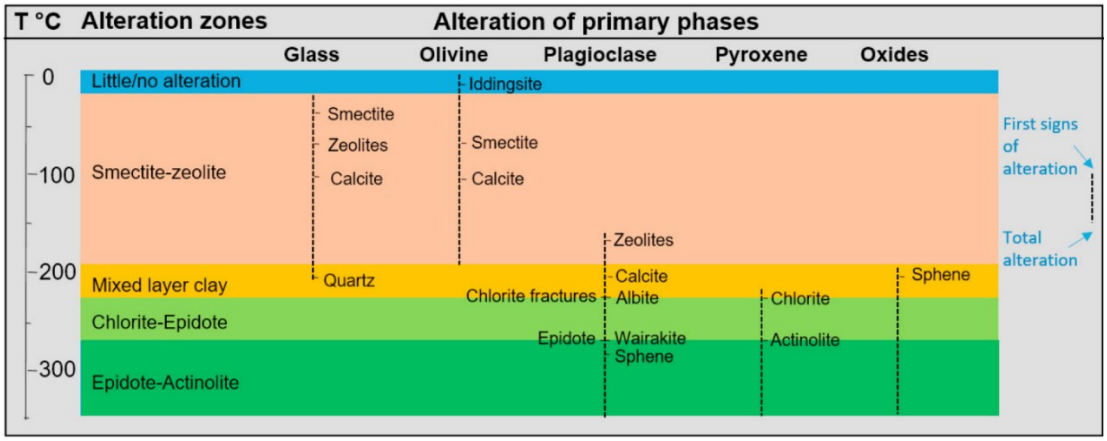

Figure 2: Alteration zones and breakdown of the primary phases at the CarbFix reinjection site (Snæbjörnsdóttir, 2018).

The geothermal wells in the Hellisheiði field, including the wells considered in this study, are cased off down to the chlorite-epidote zone. The host rock of the geothermal field and the CarbFix reservoir is therefore affected by high temperature alteration (>230 °C). The formation of secondary minerals corresponds with the breakdown of primary phases: volcanic glass, olivine, plagioclase, pyroxene, and oxides (Snæbjörnsdóttir *et al.* 2018). At reservoir depth volcanic glass and olivine in the host rock were found to be fully altered. The alteration products of volcanic glass include clay minerals, zeolites, calcite, and quartz (Snæbjörnsdóttir *et al.* 2018). Olivine usually forms calcite and smectites, which alter at high temperatures to chlorites. Alteration of plagioclase to zeolites, chlorite (230->300°C), albite, calcite, epidote (>230-250°C) and wairakite (>200°C) has been identified in wells both at Skarðsmýrarfjall and near well HN-16. Similarly, alteration products of pyroxene, chlorite (>230°C) and actinolite (>280°C) are present (Snæbjörnsdóttir, 2011).

Binocular microscope analysis of drill cuttings and thin section analysis of drill cuttings from the wells considered in this study and other wells in the immediate vicinity show that chlorite is the most common alteration mineral in the study area (Snæbjörnsdóttir, 2011). Calcite is also common in the Hellisheiði field, and is expected to form at temperatures below 300°C. The other minerals present are believed to include primary phases (pyroxenes, feldspar, and oxides) and silicates of secondary origin (quartz and epidote).The mineralogy of the rock formation in the CarbFix reservoir is a complex equilibrium between minerals of primary and secondary origin which evolves with increasing depth and temperature.

3. THE CARBFIX PROJECT

The CarbFix project, which is co-funded by the EU, is a combined industrial and academic research project centred on the Hellisheiði power plant. The project developed methods and technology for the permanent mineral storage of CO_2 and CO_2-H_2S gas mixtures in basalts. The CarbFix method has been extensively reported on and readers are directed to Sigfússon et al. (2015, 2018) and Gunnarsson *et al.* (2018) for a complete description of the capture and sequestration process.

3.1 CarbFix: an integrated carbon and sulfur capture and sequestration process

The CarbFix method consists of soluble gas mixture capture in water followed by the direct injection of the resulting CO2-H2S-charged water into basaltic rock. In 2012, two pilot-scale injections were carried out in Hellisheiði where 175 tons of CO2 and 73 tons of a gas mixture consisting of 75% CO2 and 25% H2S from the Hellisheiði power plant were injected, respectively (Sigfússon et al. 2015). Extensive geochemical monitoring revealed the rapid mineralization of the injected gases: over 95% of the injected CO2 was mineralized in less than two years and the bulk of the injected H2S was mineralized within four months from injection (Matter et al. 2016, Snæbjörnsdóttir et al., 2017). Following the success of the two pilot scale injections, the CarbFix method was scaled up as part of the industrial scale injections starting in June 2014. Research in the currently EU funded CarbFix2 project is related to this upscaled injection. A CO2 and H2S dominated gas mixture is captured from the Hellisheiði power plant exhaust gas stream by its dissolution into pure water in a scrubbing tower (Aradottir et al. 2015).The average composition of the water leaving the scrubbing tower contained 102 mmole/kg dissolved inorganic carbon (DIC) and 72.9 mmole/kg dissolved sulfur (DIS) with an average pH of 3.5 (Table 1, Figure 3). In July 2016 the scrubbing tower was optimized to recover 56% of the CO2 and 97% of the H2S from the

exhaust stream. The percentage of CO2 and H2S recovered was increased by increasing the pressure in the scrubbing tower and the resulting mixture contains 160 mmole/kg of DIC and 102 mmole/kg of DIS (Table 1, Figure 3).

The pressurized gas-charged water is transported via a 1.5 km long pipe to the HN-16 injection well, where it is injected into the subsurface. The injection rate was 30 to 36 kg/s (Figure 3), such that a total of 14.5 tons CO_2 and 7.9 tons H_2S were injected each day (Sigfússon *et al.* 2018). The separated water had a temperature ranging from 55 to 140 °C, with an average pH of 9.13 (Table 3), and was injected at a rate of 15 to 130 kg/ s (Figure 3). Well HN-16 was retrofitted to receive the gas-charged condensate from the CarbFix capture plant; a stainless-steel pipe was added to receive the gas mixture (Figure 4). The separator water flows on the outside of the stainless-steel pipe to avoid contact between the acidic (and corrosive) the gas-charged condensate and the carbon steel casing. The two fluids mix at the exit of the stainless-steel pipe at a depth of 750 m (approximately -400 masl).

3.2 The CarbFix timeline

Operations at the CarbFix2 reinjection site started in August 2011 and can be divided into seven successive stages (Figure 3):

1. In September 2011, well HN-16 was put online and connected to the geothermal separated water disposal as part of the operations at the Hellisheiði power plant. A portion of the seal water (gas-enriched condensate used to extract the NCGs from the condenser in the liquid ring vacuum pumps) is fed in a closed circuit towards the re-injection wells of the power plant (Sigfússon et al. 2018). The chemistry of the separated water presented in the study is sampled after the seal water is fed into the reinjection stream and mention of the separated water represent the separated water mixed with the seal water (Table 1).
2. Commissioning of the CarbFix capture plant, separated water and pure condensate reinjected in HN-16 (Figure 1).
3. Injection of the CarbFix water (gas enriched condensate and separated water). The gas-enriched mixture contains on average 1/3 H2S and 2/3 of CO2.(Figure 3, Table 1) From 2015 a higher proportion of seal water was injected to the separated water, which lowered the pH of the separated water injected in HN-16 (Table 1)
4. Maintenance and upgrade of the surface installations. The CarbFix fluid was injected into HN-14 during this time.
5. Mixture of separator water and condensate (CarbFix water) from capture plant with one compressor on.
6. Mixture of separator water and condensate (CarbFix water) from capture plant with two compressors on allowing a sharp increase in the concentration of dissolved CO_2 and H_2S in the condensate water; from 102 to 160 mmole/kg and from 73 to 102 mmole/kg respectively. The ratio between CO_2 and H_2S remained constant (Figure 3).
7. Mixture of separator water and condensate from capture plant with two compressors on. The lowering of the condensate mass flow is because approximately 2/3 of the CarbFix water is used for pH modification of the separator water.

The work presented here will focus of the in initial injection of the CO_2 and H_2S from July 2014 to July 2015. We included the separated water injection prior the CarbFix injection from September 2011 to July 2014 as this impacts the reservoir fluid in place, rock alteration, and reservoir condition. For simplification purposes, the injection of pure condensate from April 2014 to May 2014 was not included.

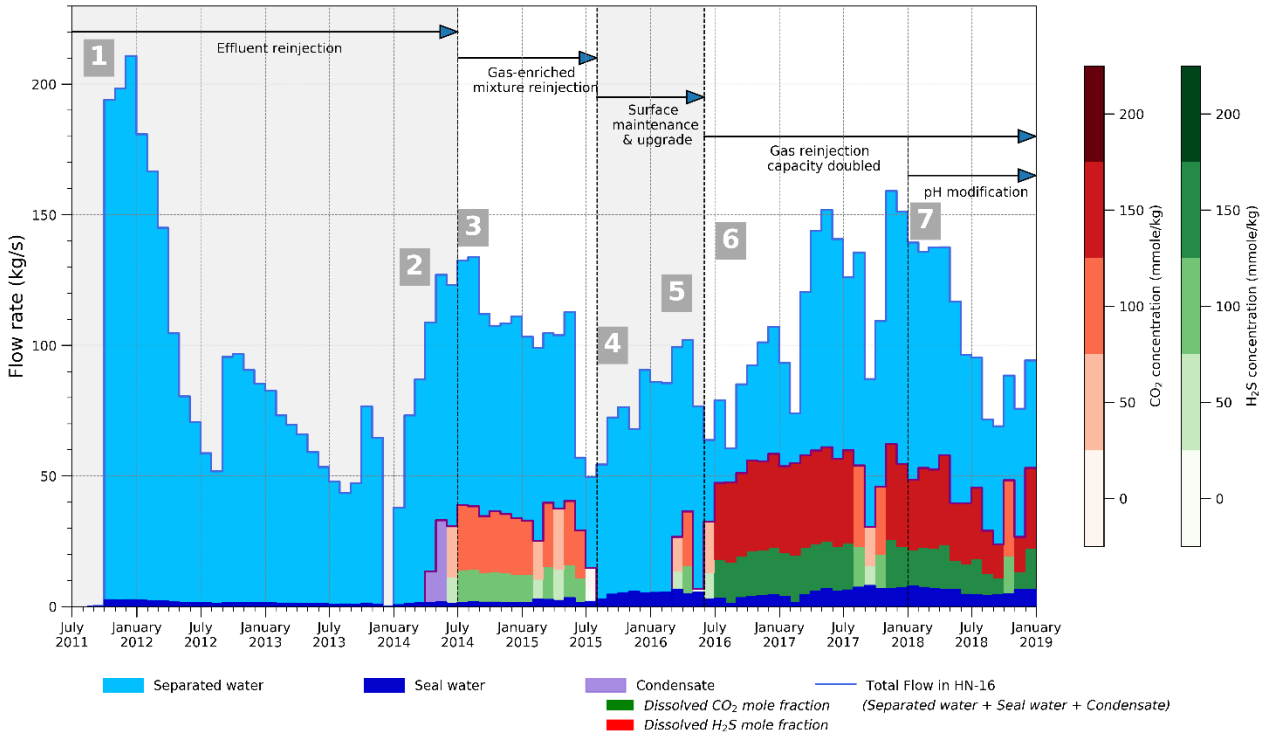

Figure 3: The CarbFix reinjection timeline. Flow rate of separator water (light blue), seal water (dark blue) and condensate water (purple) of variable gas concentrations into well HN-16 from 2011 - 2018. Dissolved mole fraction of CO_2 (red) and H_2S (green) are represented as a fraction of the condensate flow into HN-16.

Table 1: Average geochemical compositions of injected separated water geothermal and gas-charged waters before and after July 2016. The average composition of the background reservoir is also given. Values given in mmol/kg and mass flow in kg/s.

Phase		***September 2011 - June 2014***	***June 2014 – July 2015***	***July 2015 – February 2016***	***February 2016 – January 2018***	***January 2018 – December 2018***
		Separated water reinjection	CarbFix water reinjection	Separated water reinjection	CarbFix water reinjection	CarbFix water reinjection
Phase description		Geothermal water disposal	Separator water & gas charged condensate mixture	Surface maintenance and upgrade – CarbFix water injected in HN-14	Increase in seal water proportion in the separated water	Acidification of the separated water
Gas-charged water composition	Mass flow		33		48.3	37.1
	Temperature		23		20.8	21.0
	pH		3.5		3.6	3.6
	CO_2		102.35		161.3	161.3
	H_2S		72.9		102.4	102.4
Separated water and reservoir fluid composition	Mass flow	88.2	76.9	72.1	63	66.5
	Temperature	74.3	66.9	65.7	63.4	63.8
	pH	9.21	9.13	9.13	7.38	6.33
	CO_2[1,2]	0.3452	0.4244	0.4244	7.3117	9.2674
	H_2S[2]	0.6378	0.4424	0.4424	5.4106	6.9264
	SO_4[1]	0.1566	0.2464	0.2464	0.5714	0.7243
	Si[3]	7.9663	8.1700	8.1700	0.0145	0.0175
	Na[3]	6.0194	6.1257	6.1257	0.0029	0.0026
	K[3]	0.6311	0.6161	0.6161	0.0002	0.0028
	Ca[3]	0.0123	0.0143	0.0143	0.0438	0.0517
	Mg[3]	0.0006	0.0004	0.0004	3.1426	4.4419
	Fe[3]	0.0004	0.0007	0.0007	0.0431	0.0535
	Al[3]	0.0464	0.0470	0.0470	1.5390	
	Cl[1]	3.3863	3.3600	3.3600	2.6422	5.4839
	F[1]	0.0426	0.0509	0.0509	0.1153	0.2053

[1]*Measured by Ion Chromatography (IC)*
[2]*Measured by Electrodes and Titration (E&T)*
[3] *Measured by Inductively Coupled Plasma mass spectrometry (ICP)*

4. MODELLING APPROACH

Numerical modelling plays an important role in the CarbFix project as it allows to model and better understand the complex behaviour of time dependent transport and fluid rock interaction in the reservoir. It also provides tools to predict and optimize long-term management of the injection site as well as to quantify the amount of CO_2 that can be mineralized. TOUGH2 (Pruess, 1991), iTOUGH2 (Finsterle, 1999) and TOUGHREACT (Xu *et al.* 2006, 2011) have been used for developing the field scale models as part of the CarbFix2 project. The workflow of the model development was divided into the following four interrelated stages:

1. Development of a conceptual model of regional hydrological flow conditions (Ratouis *et al.,* 2018),
2. Flow model to estimate the hydrological parameters constrained by model calibration to field data (tracer test and flowing enthalpy recorded in the monitoring well) (Ratouis et., al 2019),
3. One-dimensional reactive transport models set at the feedzone depth of the injection well,
4. Predictive model simulations with a three-dimensional field scale fully coupled reactive mass transport model, and model validation by comparison to field data.

Ratouis *et al.,* (2019) and Ratouis *et al.,* (2020) discuss in detail the conceptual model of the CarbFix injection site at Husmuli, and the hydrological parameters constraint by the flow models calibrated with the tracer test results. This work focuses on the development of one-dimensional reactive transport models to constrain the complex geochemical process involved with CO_2/H_2S mixture injection in a basaltic host rock under reservoir conditions. The benefit of this approach is to avoid the added complexity of the increasing state of alteration of the host rock with depth and vertical flow of the hydrothermal flow. As a first approach, this allows us to focus on the impact of gas-charged fluid mixture injection on the altered host rock. This also allows us to test and compare the reactive transport at various depth and temperature conditions and to validate the thermodynamic database (Voigt *et al.*, 2018). The aim of this work is to be incorporated into the three-dimensional flow model of the CarbFix reinjection site once the relevant geochemical reactions are better constrained.

4.1 Conceptual model

The Husmuli area has been utilised for the reinjection of separated geothermal water and pressure support in the geothermal reservoir as part of the operations at Hellisheiði since 2011. The injected fluid enters the reservoir through feed-zones of the open section of the injection well. In volcanic rocks the feed-zones are often fractures or permeable layers such as interbeds. At Hellisheiði the permeable zones below the cased section have been linked to open fractures and major faults (Thordarson *et al.* 2011). In HN-16 three main feedzones or area of high permeability have been identified using televiewer and internal drilling reports (Ratouis *et al.*, 2019). Our conceptual model of the CarbFix reservoir considers one-dimensional flow tube between the feedzones of the injection well and monitoring wells, which should be considered as a small sub-volume of a much more extensive 3-D reservoir. From the injection side to the production side, the model consists of 2000 one metre grid blocks. Hydrological parameters used in the present simulations are listed in Table 2.

Table 2: Hydrological parameter

Rock	Density (kg/m^3)	Porosity	Permeability (m^2)	Conductivity (J/kg K)	Specific heat (J/kg K)
Altered basalt	2600	0.15	1 10^{-12}	1.5	900

The modelling approach has been expanded to include The CarbFix injection method by integrating the horizontal reservoir models with a simple one-dimensional vertical model to represent the wellbore and mixing process within the injection well (Figure 4). The mixing model consists of 1400 blocks and extends from the outlet of the stainless-steel to the bottom of the well. The mixing of the fluid is simulated using the option in TOUGHREACT to only solve flow and transport without chemical reaction. At the top of the wellbore model in one element the separated water of known chemistry composition with a fixed flow rate is injected and in the neighbouring block the gas-enriched condensate (fixed flow rate) presented in Table 1 (Figure 4). The simulation is run for 10 days enough to have a complete mixing of the separated water and the gas-enriched condensate. The resulting fluid mixing is then extracted from the model at the feedzones depth. The mixing of the fluid is complete before first feedzones at -700 masl is reached. Therefore, the chemistry of the mixture is very similar for all feedzones (slight difference due to the increasing pressure within the wellbore with depths). The fluid at the different feedzones is then injected in the one-dimensional models representing the CarbFix reservoir. The one-dimensional models simulate the reinjection from October 2011 to July 2015 using the values shown in Figure 3. As mentioned above two distinct phases are considered in this work; the separated water injection from October 2011 and the CarbFix gas-enriched mixture injection from June 2014 to July 2015 before the gas capture system was upgraded.

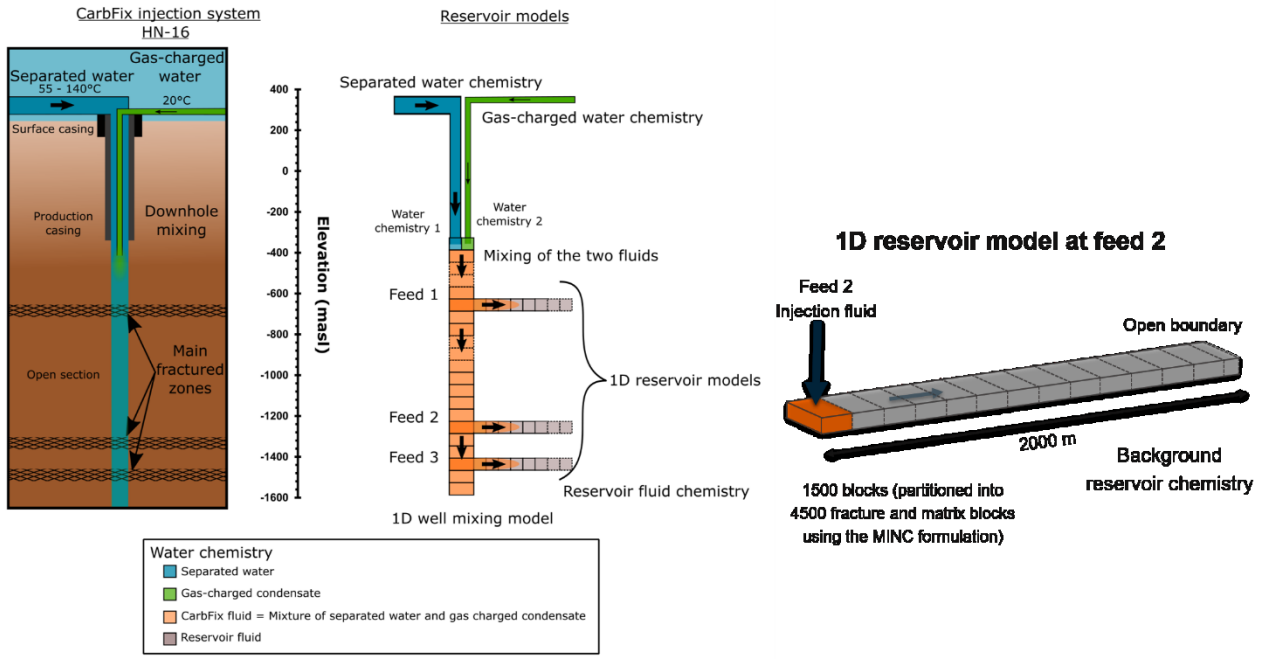

Figure 4: Left: Schematic diagram of the injection system, from the fluid inlets at the well head to the outlet within the reservoir. Within the casing of the well is a stainless-steel pipe that reaches 750 m, thus preventing any contact between the carbon steel and the gas-charged water. The two fluids, separated water and gas-charged water, were injected separately, mixing at the exit of the stainless-steel pipe. The three feedzones receiving the water mixture are located at elevations comprised between -700 and -1500 masl with a temperature of 220 – 260 °C. Right: Integrated reservoir models of the fluid mixing and one-dimensional models of the target reservoir located at the permeable fractures intersected by HN-16.

4.2 Background chemistry and mineralogy

The background chemistry of the reservoir was determined by calculating the average chemistry of the monitoring wells before the start of injection at the Husmuli site. Three samples were available for HE-31, and two samples for wells HE-48 and HE-44. The average chemistry is given in Table 3. This will be used as the initial water composition of the background water used in the simulations. Initial mineralogical composition of the mineral phase is given in Table 4. The mineral assemblage represents strongly altered olivine tholeiitic basalts describe in section 2.2.

Table 3: Reservoir fluid chemistry. Values given in mmol/kg. Average fluid composition sampled from HE-31, HE-48, HE-44, and HE-33 before 2011

	Background reservoir composition
pH	7.12
CO_2[1,2]	19.5312
H_2S[2]	2.0242
SO_4[1]	0.5807
Si[3]	8.9254
Na[3]	5.7182
K[3]	0.6028
Ca[3]	0.0194
Mg[3]	0.0002
Fe[3]	0.0002
Al[3]	0.0802
Cl[1]	1.9967
F[1]	0.0968

[1]*Measured by Ion Chromatography (IC)*
[2]*Measured by Electrodes and Titration (E&T)*
[3] *Measured by Inductively Coupled Plasma mass spectrometry (ICP)*

Table 4: Initial rock mineral composition

	Phase	*Group*	*Volume % of solid*	*Mineral*	*Volume % of solid*	*Area (cm^2/g)*
Initial rock mineral composition	**Primary mineralogy**	**Pyroxenes**	0.1	Ca,Al Pyroxene	0.02	2
				Diopside	0.02	2
				Hedenbergite	0.02	2
				Ferrosilite	0.02	2
				Enstatite	0.02	2
		Feldspars	0.1	Albite	0.05	2
				K-Feldspar	0.05	2
		Fe oxy-hydroxides	0.1	Hematite	0.05	100
				Magnetite	0.05	100
	Secondary Mineralogy	**Carbonates**	0.1	Calcite	0.1	
		Chlorites	0.4	Chamosite	0.2	2
				Clinochlore	0.2	2
		Other silicates	0.1	Quartz	0.1	2
			0.1	Epidote	0.1	2

The minerals considered in this study listed in Appendix A with the formation reaction and the stability field (when available). They include a wide range of secondary minerals stable at various reservoir condition that may be encountered in the simulations. Carbonates, Sulfur bearing minerals, Clay minerals, Chlorites, Zeolites, other silicates, and Kaolins, have all been considered in this study. Solid solutions were considered for Magnesite-Siderite mineral series, Saponite, Montmorillonite, and Chlorites end members (Appendix A).

Dissolution and precipitation of all minerals is kinetically controlled. Kinetic rates are a product of the rate constant and reactive surface area, according to the following general rate expression, which is transition state theory based (Lasaga *et al.* 1994; Steefel and Lasaga, 1994):

$$r = kA\left[1 - \left(\frac{Q}{K}\right)^{\theta}\right]^{\eta} \quad (1)$$

where r is rate of dissolution or precipitation, k is the temperature dependent rate constant, A is the specific reactive surface area, K is the equilibrium constant for the dissolution/precipitation reaction taking place and Q is the reaction quotient. θ and θ must be determined by experiment but are often set to unity. The kinetic rate expression of different minerals used in the simulation can be found in Appendix B. Mineral reactive surface areas in the subsurface are generally unknown. In the current study, reactive surface area of primary minerals and glasses was assumed to be 2-100 cm2/g, in agreement with the work of Sonnenthal et al. (2005). Surface areas of precipitating minerals are generally much higher than those of the primary rock. In the current study, surface areas of secondary clay minerals, zeolites and carbonates were assumed to be 10,000, 1000 and 500 cm2/g, respectively. Secondary SiO2(s) minerals were assumed to have a surface area of 1000 cm2/g. When the aqueous phase supersaturates with respect to a certain secondary mineral, a small volume fraction of 1×10−6 is used for calculating a seed surface area for the new phase to grow (Xu *et al.* 2010). The precipitation of secondary minerals is represented using the same kinetic expression as that for dissolution, except for SiO2(am) which precipitates under the free energy rate law of Carroll et al. (1998). As precipitation rate data for most minerals are unavailable, parameters for neutral pH rates were employed to describe precipitation.

5. SIMULATIONS

5.1 Framework

Batch geochemical simulations of water-rock interaction were carried out before starting fully coupled reactive mass transport simulations in order to pre-react the average background water composition to a steady state with the minerals (listed in Table 4) under reservoir conditions. The TOUGHREACT simulator then solves fluid and heat flow equations as well as equations describing

chemical reactions in every model block in the one-dimensional simulations. Simulations were carried out for the three horizontal one dimensional models from October 2011 to July 2015. The results presented below are from the one-dimensional model for feed 2 at a depth of -1300 masl and an initial reservoir temperature of 240°C.

5.2 Simulation results

Prior to the CarbFix mixture, cooled separated water, an alkaline solution with a pH 9.13 is injected into the reservoir. The modelled temperature distribution and pH change are shown in Figure 5. The model results will be used as the initial condition for the gas-charged injection from June 20th, 2014.

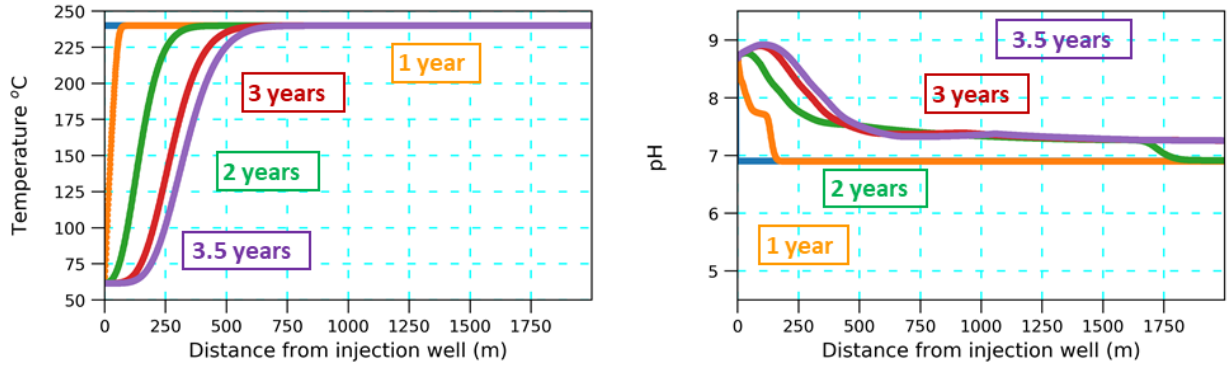

Figure 5: Model results from September 2011 to June 2014 – Cool alkaline CO_2/H_2S depleted water injection. Temperature (left) and pH (right) versus distance at different times during the separated water injection prior to the CarbFix injection.

The gas-charged condensate is added to the separated water using the injection system shown in Figure 4. The resulting fluid has a pH of 4.9 and is injected in the reservoir model (Figure 6). The gradual change in pH can be seen in Figure 6.

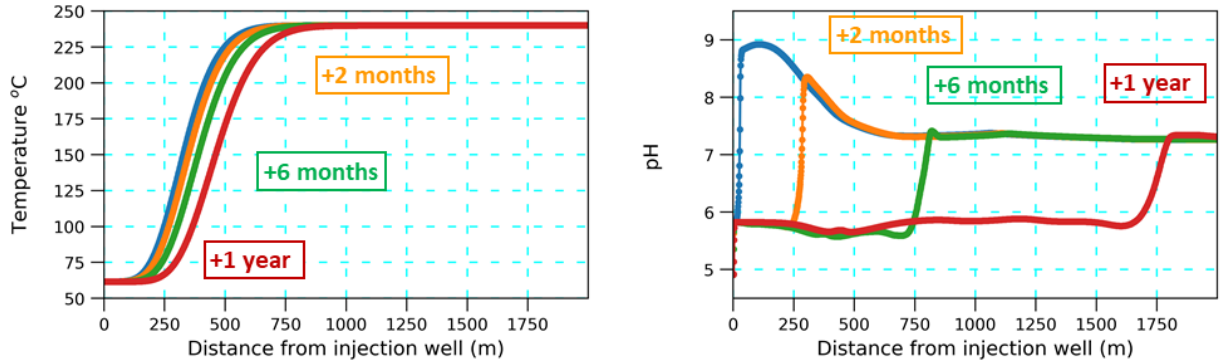

Figure 6: Model results from June 2014 to July 2015 – Cool acidic gas-charged mixture injection. Temperature (left) and pH (right) versus distance at different times during the CarbFix injection.

From left to right Figure 7 shows the concentration of Calcium and Iron, DIC and DIS and changes in volume fraction of carbonates and sulfur bearing minerals along the x-axis of the reservoir at different times during the CarbFix injection. This plot illustrates the CarbFix mineralization process in the reservoir: as the weakly acidic fluid (pH = 4.9) enters in the reservoir and interacts with the host rock and dissolution of minerals occur, leaching cations out of the rock matrix and increasing the pH up to value around 6. As dissolution reactions proceed concentration of leached cations builds up (left in Figure 7). At certain concentrations, the water becomes supersaturated with respect to secondary minerals including carbonates and sulfur bearing minerals, which begin to precipitate (right in Figure 7). An additional mechanism comes also into play for carbonates precipitation; the retrograde solubility of calcite. This will limit precipitation of calcite in the area affected by the temperature decline in the vicinity of the injection. Calcite will preferentially precipitation as the reinjected fluid is being heated by the reservoir (Figure 8). Figure 8 shows that in the area that is cooled down precipitation of ankerite occurs. Pyrite is oversaturated very close to the wellbore, then again gradually further along the flow path. Simulations indicated no precipitation of other carbonates such as magnesite or siderite and no anhydrite.

Figure 9 shows that the precipitation of calcite and pyrite will compete for cations with precipitation of clays, chlorites, and epidotes. Clays forms exclusively at low temperatures closer to the reinjection well and chlorites and epidotes will form at the higher temperatures.

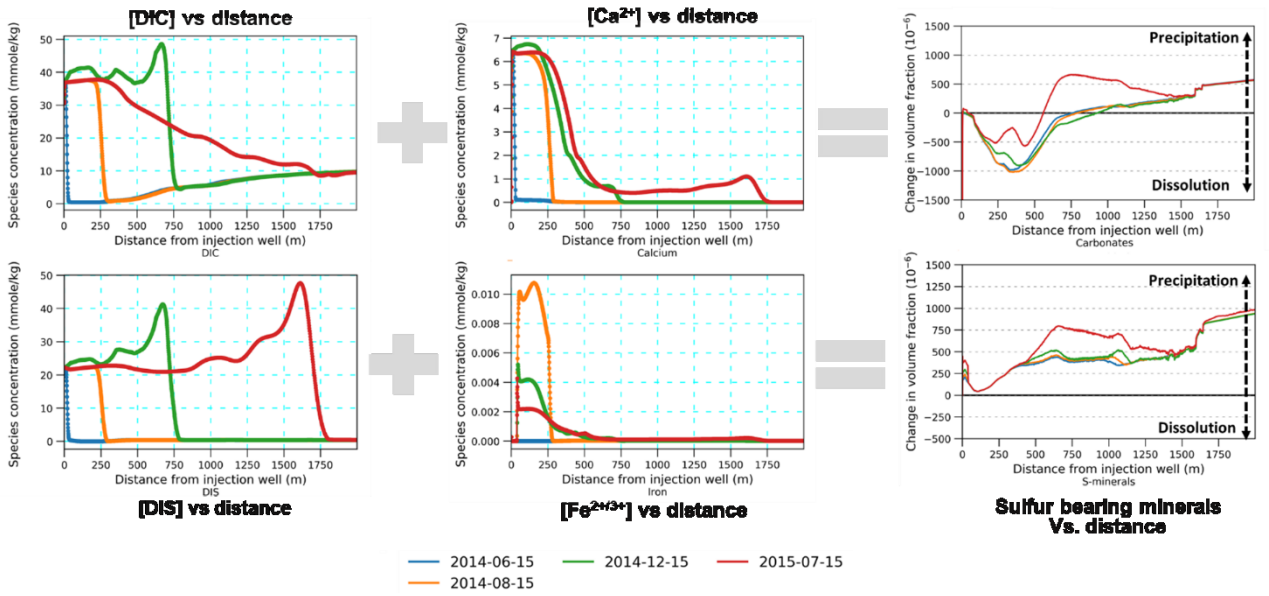

Figure 7: Model results from June 2014 to July 2015 – Concentration of Calcium, Iron, DIC, and DIS and changes in volume fraction of carbonates and sulfur bearing minerals along the x-axis of the reservoir.

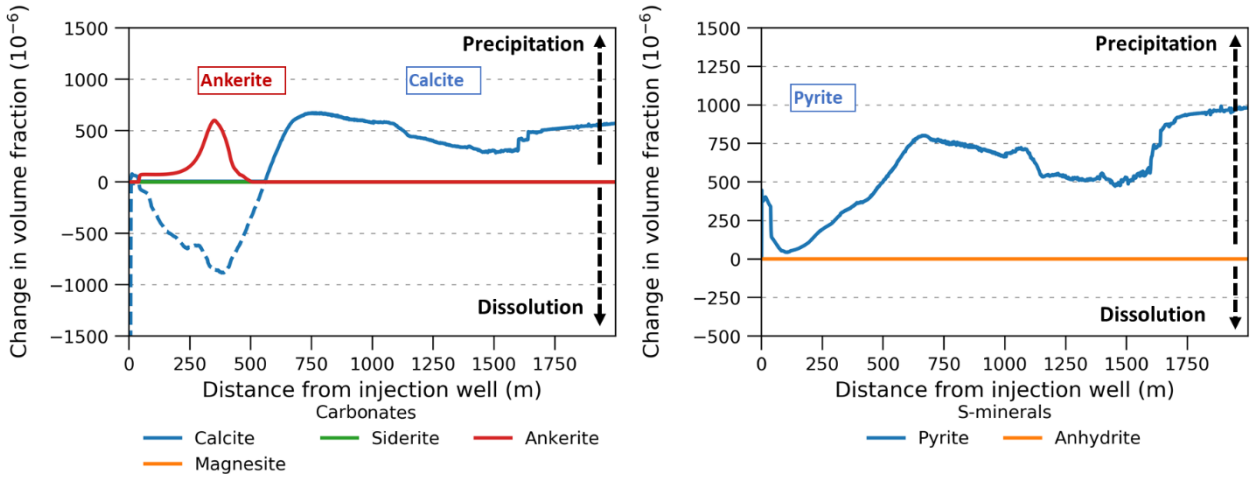

Figure 8: Model results – Change in volume fraction for carbonates (left) and sulfur bearing minerals (right) vs. distance at the end of the CarbFix injection.

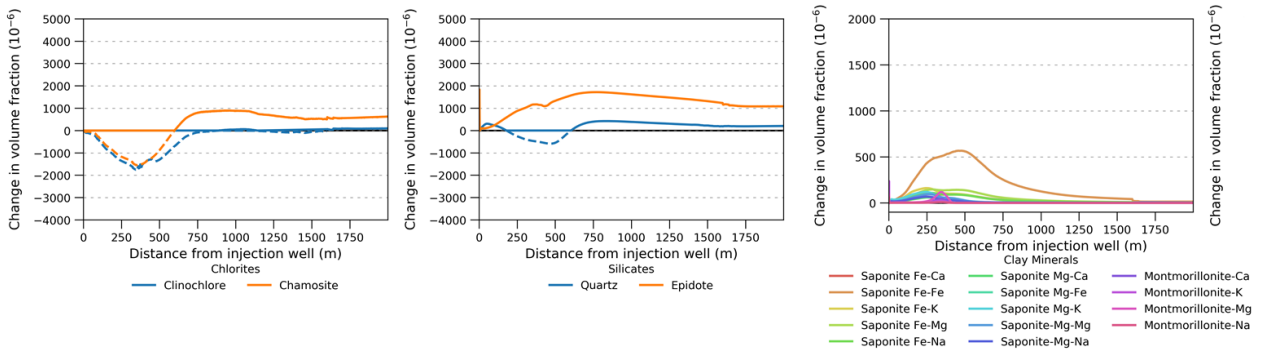

Figure 9: Model results – Chlorites (left) and Silicates (middle), and Clay minerals (left) versus distance at the end of the CarbFix injection.

Figure 10 shows a slice view along the x-axis of the 1D reservoir showing the temperature, pH, carbonates and sulfur-bearing mineral distribution after 6 month of injection (November 2014) and at the end of the CarbFix injection (July 2015). It highlights the speed difference between the thermal front and the chemical front. The monitoring wells are shown in Figure 10, this illustrates the ability of reactive transport simulations to explore the blind side of the reservoir between the injection well and the first monitoring wells where many changes in the reservoir are expected but no direct measurement can be retrieved.

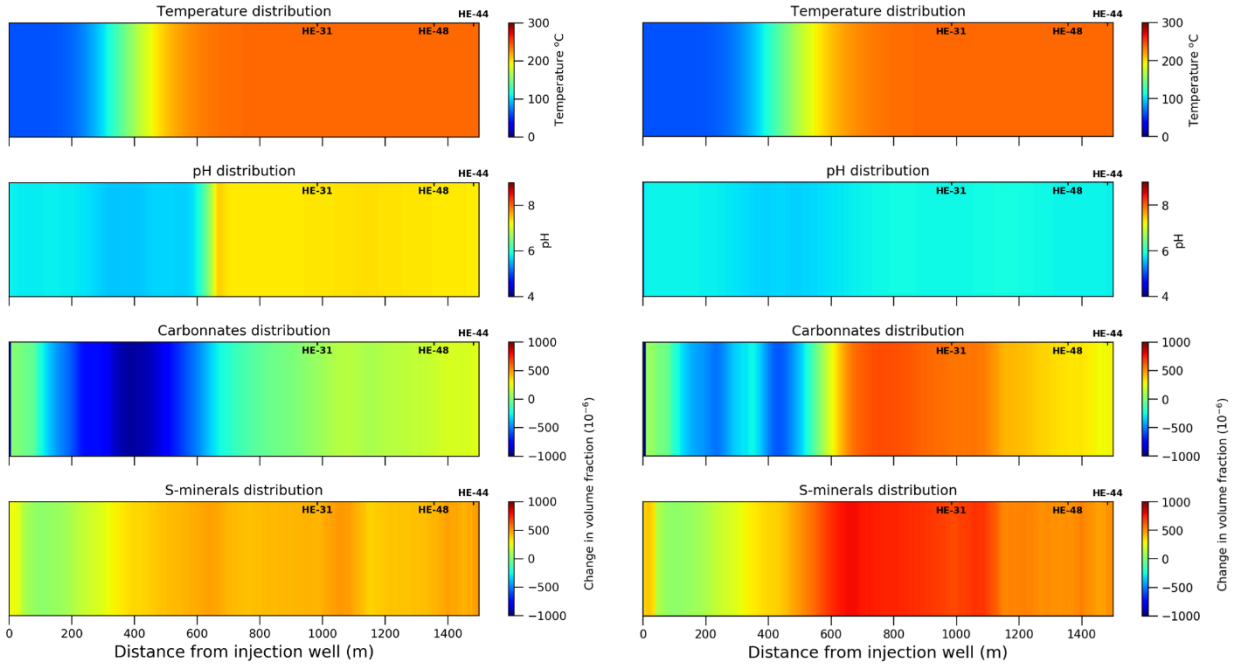

Figure 10: Slice view along the x-axis of the 1D reservoir showing the temperature, pH, carbonates and sulfur-bearing mineral distribution after 6 month of injection (November 2014) and at the end of the CarbFix injection (July 2015).

Figure 11 shows the changes in porosity at different time along the x-axis of the reservoir. Model results predict an increase in porosity (+5%) in the vicinity of the reinjection well caused by mineral dissolution (mainly calcite) by the weakly acidic fluid injected into the reservoir. This is supported by field observations, well injectivity have remain stable or slightly increased during the CarbFix injection. Clogging around the wellbore is therefore not expected, the bulk of the carbonates and sulfur bearing minerals happens at a distance from the injection well. The model also shows that the porosity reduction along the flow path is limited (-0.2%) and the space available for mineral precipitation is greater than the bulk volume of mineralization.

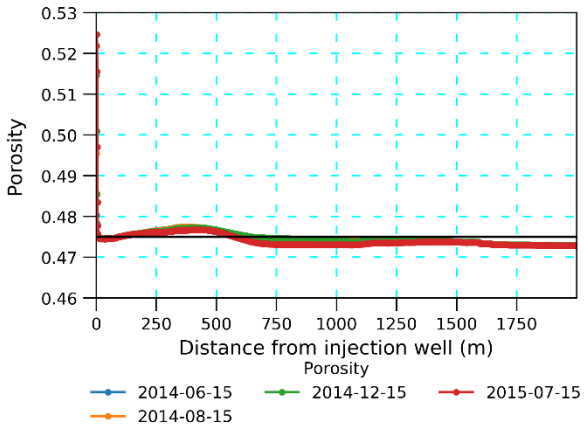

Figure 11: Model results from June 2014 to July 2015 – Porosity changes in the reservoir.

Figure 12 compares change in volume fraction for carbonates, sulfur bearing mineral, chlorites, and epidotes at various reservoir temperatures. The largest amount of CO_2 is precipitated at 240°C. The efficiency of the carbon trapping mechanism increases with temperature from 200°C to 240°C, then drops for temperatures above 240°C. This effect has been suggested by Gunnarsson *et al.*, (2018) stating that while the rates of basalt dissolution and of mineral carbonation reactions increase with temperature it will be offset by the decreasing thermodynamic drive for carbonate mineral formation with increasing temperature. Calcite and quartz decompose into wollasonite, liberating CO_2 at temperatures exceeding 325°C. It is worth noting that the optimum temperature for carbon sequestration predicted in this study is substantially higher than the optimum temperature of 185 °C proposed by Gunnarsson *et al.*, (2018). Many factors may contribute to an optimum reservoir target temperature and should better understood and constrained in future studies. The efficiency of H_2S mineralization on the other hand increases with higher temperature with the largest volume of pyrite formed at temperatures of 260°C and above.

It is also important to consider the effect of temperature on the competing mechanism which can hinder or increase the efficiency of the trapping mechanisms. The simulation shows that the amount of chlorite dissolution increases with temperatures which will provide cations for the mineralization processes. An opposite behavior is predicted for epidote; precipitation increases with temperature which will compete for cation availability with carbonates and pyrite formation.

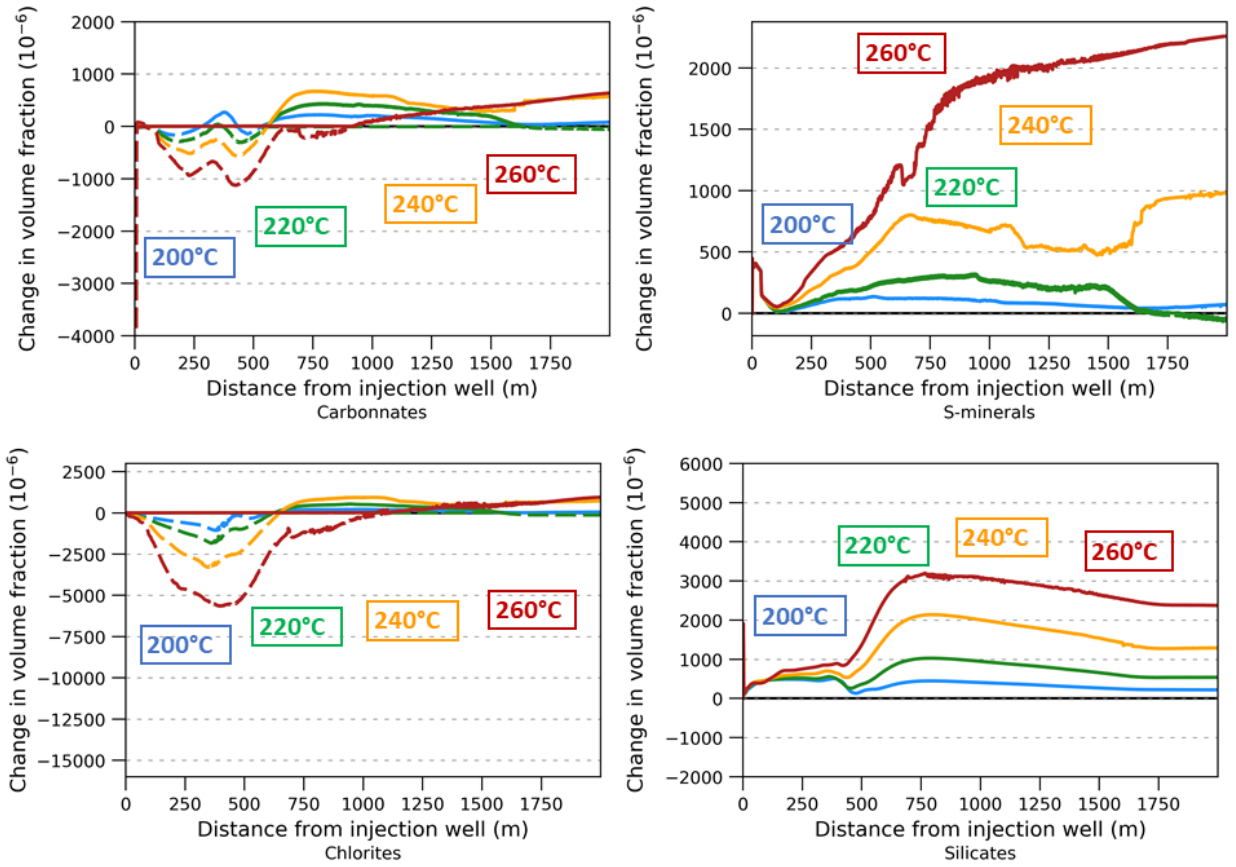

Figure 12: Model results at the end of the CarbFix injection (July 2015) – Change in volume fraction along the x-axis of the 1D reservoir for different initial reservoir temperature.

5. SUMMARY AND CONCLUSIONS

This paper describes the different stages of the CarbFix injection and provides an up-to-date timeline of the implementation of the CarbFix technology at the Husmuli reinjection site. It highlights the ongoing commitment of the CarbFix team to develop, improve, and optimize the capture and sequestration processes of greenhouse gases at the Hellisheiði power station.

The reactive transport simulations carried out in this study indicate in situ CO_2/H_2S mineral sequestration in altered basalt is viable at temperature ranging from 220-260°C. The models show that injected carbonated/sulfurized water is capable of leaching cations from the basaltic rock matrix. This eventually results in pore water becoming super-saturated with respect to carbonates (mainly calcite) and pyrite, into which CO_2 and H_2S is sequestered. It also predicts that the mineralization process occurs at a distance from the injection well, suggesting that clogging in its near vicinity is not likely as postulated by Gunnarsson *et al.*, (2018). We were able to identify competing mechanisms including silicates and clay precipitation which could impact adversely mineral sequestration processes. This modelling study used a new high temperature thermodynamic database compiled by University of Iceland (CarbFix database). The database was converted from a Phreecq to a format readable by the TOUGHREACT simulator.

The one-dimensional modelling study undertaken in this work is qualitative and will need to be improved and compared against the monitoring data available in the future. Furthermore, the one-dimensional model provided a robust tool to test the thermodynamic database. The one-dimensional model and single flow channel representation of the reservoir does not accurately represent flow in the Husmuli area; tracer data shows the injected fluid takes 15 days to reach the first monitoring well (Ratouis *et al.*, 2019), a behaviour not replicated here. Additionally, the flow path of the fluid is not horizontal, modelling studies show that the injected fluid sinks in the vicinity of the injection well before rising as it heats up highlighting the limit of a one-dimensional approach. The reactions kinetics of mineral alteration and the impact and evolution of reactive surface areas contain high uncertainty and sensitivity studies on these parameters should be performed in future work.

ACKNOWLEDGEMENTS

We acknowledge funding from the European Commission through the CarbFix2 project (European Union's Horizon 2020 research and innovation program under grant number 764760), and S4CE (European Union's Horizon 2020 research and innovation program under grant number 764810). We thank our friends in the CarbFix group, our colleagues at the R&D department at Reykjavik Energy for their contribution to this work.

REFERENCES

Aradóttir, E.S.P., Sigfússon, B., Snæbjörnsdóttir, S.O., Arnarson, M.Þ., Ratouis, T.M.P., Helgason, K., Bragadóttir, R.B., Clark, D., Marieni, C., Voigt, M., Gunnlagsson, E., Oelkers, E., Gíslason, S.R.: CarbFix – Climate Action by Turning CO2 to Stone. *Proceedings*. World Geothermal Congress, Reykjavik, Iceland (2020).

Broecker, W.: Climate change: CO_2 arithmetic. Science 315, (2007), 1371.

Franzson H., K. Arnason, K. Sæmundsson, B. Steingrimsson, B.S. Hardarson, and E. Gunnlaugsson.: The Hengill geothermal system, conceptual geological model. Proceedings, World Geothermal Congress, Bali, Indonesia (2010).

Gunnarsson, I., Aradóttir, E.S., Oelkers, E.H., Clark, D.E., Arnarson, M.Þ., Sigfússon, B., Snæbjörnsdóttir, S.Ó., Matter, J.M., Stute, M., Juliusson, B.M., Gislason, S.R.: The rapid and cost-effective capture and subsurface mineral storage of carbon and sulfur at the CarbFix2 site. International Journal of Greenhouse Gas Control 79 (2018) 117–126.

IEA.: 20 years of carbon capture and storage – accelerating future deployment. International Energy Agency, Paris, France (2016).

Khodayar M., Axelsson G., Steingrímsson B. Potential Structural Flow Paths for Tracers and Source Faults of Earthquakes at Húsmúli, Hengill, South Iceland. *Report ÍSOR-2015/035* (2015).

Kristjánsson B.R., G. Axelsson, G. Gunnarsson, I. Gunnarsson, and F. Óskarsson.: Comprehensive Tracer Testing in the Hellisheiði Geothermal Field in SW-Iceland, Proceedings, 41st Workshop on Geothermal Reservoir Engineering, Stanford, California (2016).

Lagat J.: Hydrothermal alteration mineralogy in geothermal fields with case examples from Olkaria domes geothermal field, Kenya. Presented at Short Course IV on Exploration for Geothermal Resources (2009).

Matter J.M., Stute, M., Snæbjörnsdottir, S.Ó., Oelkers, E.H., Gislason, S.R., Aradottir, E.S., Sigfússon, B., Gunnarsson, I., Sigurdardottir, H., Gunnlaugsson, E., Axelsson, G., Alfredsson, H.A., Wolff-Boenisch, D., Mesfin, K., Taya, D.F. de la R., Hall, J., Dideriksen, K., Broecker, W.S.: Rapid carbon mineralization for permanent disposal of anthropogenic carbon dioxide emissions. Science 352, (2016), 1312-1316.

Metz, B., Davidson, O., de Coninck, H., Loos, M., Meyer, L.: IPCC Special Report on Carbon Dioxide Capture and Storage. Cambridge University Press, New York (2005).

Ratouis, T.M.P., Snæbjörnsdóttir, S.O., Gunnarsson, G., Gunnarsson, I., Kristjánsson, B.R., Aradóttir, E.S.P.: Modelling the Complex Structural Features Controlling Fluid Flow at the CarbFix2 Reinjection Site, Hellisheiði Geothermal Power Plant, SW-Iceland. Proceedings, 44th Workshop on Geothermal Reservoir Engineering, (2019).

Ratouis, T.M.P., Snæbjörnsdóttir, S.O., Gunnarsson, G., Gunnarsson, I., Aradóttir, E.S.P.: Modelling the Flow Paths at the Carbfix2 Reinjection Site, Hellisheiði Geothermal Power Plant, SW-Iceland. Proceedings World Geothermal Congress, (2020).

Schrag, D.: Preparing to capture carbon. Science 315, (2007), 812–813.

Sigfússon B., Gislason, S.R., Matter, J.M., Stute, M., Gunnlaugsson, E., Gunnarsson, I., Aradottir, E.S., Sigurdardottir, H., Mesfin, K., Alfredsson, H.A., Wolff-Boenisch, D., Arnarsson, M.T., Oelkers, E.H.: Solving the carbon-dioxide buoyancy challenge: The design and field testing of a dissolved CO_2 injection system. International Journal of Greenhouse Gas Control 37, (2015).

Sigfússon, B., Arnarson, M.Þ., Snæbjörnsdóttir, S.Ó., Karlsdóttir, M.R., Aradóttir, E.S., Gunnarsson, I.: Reducing emissions of carbon dioxide and hydrogen sulphide at Hellisheiði power plant in 2014-2017 and the role of CarbFix in achieving the 2040 Iceland climate goals. Energy Procedia Volume 146, (2018) 135-145.

Sonnenthal, E., Ito, A., Spycher, N., Yui, M., Apps, J., Sughita, Y., Conrad, M., Kawakami, S.: Approaches to modeling coupled thermal hydrological and chemical processes in the Drift Scale Heater Test at Yucca Mountain. Int. J. Rock Mech. Min. Sci. 42, (2015), 684–719.

Sonnenthal, E., Spycher, N., Xu, T., Zheng L: A parallel simulation program for non-isothermal multiphase geochemical reactive transport. TOUGHREACT V3.6-OMP reactive transport user guide. Energy Geosciences Division, Lawrence Berkeley National Laboratory, California, USA (2018).

Snæbjörnsdóttir S.Ó.: The Geology and Hydrothermal Alteration at the Western Margin of the Hengill Volcanic System. MSc thesis, University of Iceland (2011).

Snæbjörnsdóttir, S.Ó., Oelkers, E.H., Mesfin, K., Aradóttir, E.A., Didersiksen, K., Gunnarsson, I., Gunnlaugsson, E., Matter J.M. Stute, M., Gislason, S.R.: The chemistry and saturation states of subsurface fluids during the in situ mineralisation of CO2 and H2S at the CarbFix site in SW-Iceland. International Journal of Greenhouse Gas Control, Volume 58, (2017) 87-102.

Snæbjörnsdóttir, S.Ó., Tómasdóttir, S., Sigfússon, B., Aradóttir, E.A., Gunnarsson, G., Niemi, A., Basirat, F., Dessirier, B., Gislason, S.R., Oelkers, E.H., Franzson, H.: The geology and hydrology of the CarbFix2 site, SW-Iceland. Energy Procedia, Volume 146, (2018) 146-157.

Steefel, C.I., DePaolo, D.J., Lichtner, P.C.: Reactive transport modeling: an essential tool and a new research approach for the Earth sciences. Earth Planet. Sci. Lett. 240, (2005) 539–558.

Thordarson, S., Blischke, A., and Franzson, H.: Hljóðsjármæling í HN-16. Short report ÍSOR-11024 (2014).

Xu, T., Sonnenthal, E., Spycher, N., Pruess, K.: TOUGHREACT – a simulation program for non-isothermal multiphase reactive geochemical transport in variably saturated geologic media: applications to geothermal injectivity and CO_2 geologic sequestration. Comput. Geosci. 32, (2006), 146–165.

Voigt, M., Marieni, C., Clark, D.E., Gislason, S.R., Oelkers E.H.: Evaluation and refinement of thermodynamic databases for mineral carbonation. Energy Procedia. 146, (2018) 81-91.

APPENDIX A

Table 5: Summary of the primary and secondary phases included in the reaction transport simulations. The composition and reaction are presented along with the mention if the minerals are considered as an ideal solid solution (as defined in Sonnenthal *et al.* 2018), and the stability field (indicative formation temperature).

Phase	*Reaction*	*Solid Solution*	*Stability field*
Primary mineralogy			
	Pyroxenes		
Ca,Al Pyroxene	$CaAl_2SiO_6 + 8H^+ = Ca^{+2} + 2Al^{+3} + SiO_2 + 4H_2O$		
Diopside	$CaMgSi_2O_6 + 4H^+ = Ca^{+2} + Mg^{+2} + 2SiO_2 + 2H_2O$		
Hedenbergite	$CaFeSi_2O_6 + 4H^+ = Ca^{+2} + Fe^{+2} + 2SiO_2 + 2H_2O$		
Ferrosilite	$FeSi_2O_6 + 2H^+ = Fe^{+2} + SiO_2 + H_2O$		
Enstatite	$MgSi_2O_6 + 2H^+ = Mg^{+2} + SiO_2 + H_2O$		
	Feldspars		
Albite	$NaAlSi_3O_8 + 4H^+ = Na^+ + Al^{+3} + 3SiO_2 + 2H_2O$		≥250 °C
K-Feldspar	$KAlSi_3O_8 + 4H^+ = K^+ + Al^{+3} + 3SiO_2 + 2H_2O$		≥250 °C
Fe oxy-hydroxides			
Hematite	$Fe_2O_3 + 6H^+ = 2Fe^{+3} + 3H_2O$		
Magnetite	$Fe_3O_4 + 8H^+ = Fe^{+2} + 2Fe^{+3} + 4H_2O$		
Secondary Mineralogy			
	Carbonates		
Ankerite	$CaFe(CO_3)_2 = Ca^{+2} + Fe^{+2} + 2CO_3^{-2}$		
Calcite	$CaCO_3 + H^+ = Ca^{+2} + HCO_3^-$		
Magnesite	$MgCO_3 + H^+ = Mg^{+2} + HCO_3^-$	1	
Siderite	$FeCO_3 + H^+ = Fe^{+2} + HCO_3^-$		
	S-minerals		
Anhydrite	$CaSO_4 = Ca^{+2} + SO_4^{-2}$		>150 °C
Pyrite	$FeS_2 + H_2O = 0.25H^+ + 0.25SO_4^{-2} + Fe^{+2} + 1.75HS^-$		
Pyrrhotite	$FeS + H^+ = Fe^{+2} + HS^-$		
	Clay minerals		
Saponite-Fe-Fe	$Fe_{3.175}Al_{0.35}Si_{3.65}O_{10}(OH)_2 + 7.4H^+ = 0.35Al^{+3} + 3.175Fe^{+2} + 3.65SiO_2 + 4.7H_2O$	2	<200 °C
Saponite-Fe-K	$K_{0.35}Fe_3Al_{0.35}Si_{3.65}O_{10}(OH)_2 + 7.4H^+ = 0.35K^+ + 0.35Al^{+3} + 3Fe^{+2} + 3.65SiO_2 + 4.7H_2O$		<200 °C
Saponite-Mg-Mg	$Mg_{3.175}Al_{0.35}Si_{3.65}O_{10}(OH)_2 + 7.4H^+ = 0.35Al^{+3} + 3.175Mg^{+2} + 3.65SiO_2 + 4.7H_2O$	3	<200 °C
Saponite-Mg-K	$K_{0.35}Mg_3Al_{0.35}Si_{3.65}O_{10}(OH)_2 + 7.4H^+ = 0.35K^+ + 0.35Al^{+3} + 3Mg^{+2} + 3.65SiO_2 + 4.7H_2O$		<200 °C
Saponite-Mg-Fe	$Fe_{0.175}Mg_3Al_{0.35}Si_{3.65}O_{10}(OH)_2 + 7.4H^+ = 0.175Fe^{+2} + 0.35Al^{+3} + 3Mg^{+2} + 3.65SiO_2 + 4.7H_2O$		<200 °C
Montmorillonite-Ca	$Ca_{0.175}Mg_{0.35}Al_{1.65}Si_4O_{10}(OH)_2 + 6H^+ = 0.175Ca^{+2} + 1.65Al^{+3} + 0.35Mg^{+2} + 4SiO_2 + 4H_2O$	4	
Montmorillonite-K	$K_{0.35}Mg_{0.35}Al_{1.65}Si_4O_{10}(OH)_2 + 6H^+ = 0.175Ca^{+2} + 1.65Al^{+3} + 0.35Mg^{+2} + 4SiO_2 + 4H_2O$		
Montmorillonite-Mg	$Mg_{0.525}Al_{1.65}Si_4O_{10}(OH)_2 + 6H^+ = 0.175Ca^{+2} + 1.65Al^{+3} + 0.35Mg^{+2} + 4SiO_2 + 4H_2O$		
Montmorillonite-Na	$Na_{0.35}Mg_{0.35}Al_{1.65}Si_4O_{10}(OH)_2 + 6H^+ = 0.175Ca^{+2} + 1.65Al^{+3} + 0.35Mg^{+2} + 4SiO_2 + 4H_2O$		
	Chlorites		
Chamosite	$Fe_5Al_2Si_3O_{10}(OH)_8 + 16H^+ = 3SiO_2 + 2Al^{+3} + 5Fe^{+2} + 12H_2O$	5	>200 °C
Clinochlore	$Mg_5Al_2Si_3O_{10}(OH)_8 + 16H^+ = 3SiO_2 + 2Al^{+3} + 5Mg^{+2} + 12H_2O$		>200 °C
	Zeolites		
Analcime	$Na_{0.96}Al_{0.96}Si_{2.04}O_6{:}H_2O + 0.92H_2O = 0.96Al(OH)_4^- + 2.04SiO_2 + 0.96Na^+$		<200 °C
Laumontite	$CaAl_2Si_4O_{12}{:}4.5H_2O = 2Al(OH)_4^- + 4SiO_2 + Ca^{+2} + 0.5H_2O$		100-200 °C
Mordenite-Ca	$Ca_{0.5}AlSi_5O_{12}{:}4H_2O = Al(OH)_4^- + 0.5Ca^{+2} + 5SiO_2 + 2H_2O$		
Stilbite-Ca	$CaAl_2Si_7O_{18}{:}7H_2O = 2Al(OH)_4^- + Ca^{+2} + 7SiO_2 + 3H_2O$		≤100 °C
Thomsonite	$Ca_2NaAl_5Si_5O_{20}{:}6H_2O + 4H_2O = 5Al(OH)_4^- + 2Ca^{+2} + 5SiO_2 + Na^+$		≤100 °C
Wairakite	$CaAl_2Si_4O_{12}{:}2H_2O + 2H_2O = 2\ Al(OH)_4^- + 4SiO_2 + Ca^{+2}$		>180 °C
	Other silicates		
Quartz	$SiO_2 = SiO_2$		
$SiO_{2\ (am)}$	$SiO_2 = SiO_2$		
Epidote	$Ca_2FeAl_2Si_3O_{12}OH + 13H^+ = Fe^{+3} + 2Al^{+3} + 2Ca^{+2} + 3SiO_2 + 7H_2O$		>200 °C
Prehnite	$Ca_2Al_2Si_3O_{10}(OH)_2 + 10H^+ = 2Al^{+3} + 2Ca^{+2} + 3SiO_2 + 6H_2O$		>200 °C
Wollastonite	$CaSiO_3 + 2H^+ = Ca^{+2} + SiO_2 + H_2O$		
	Kaolins		
Kaolinite	$Al_2Si_2O_5(OH)_4 + 6H^+ = 2Al^{+3} + 2SiO_2 + 5H_2O$		>200 °C

APPENDIX B

Table 6: Kinetic rate parameters for mineral dissolution and precipitation.

Mineral		*Parameter for kinetic rate law*							
Initial rock mineral composition	*Area*	*Neutral mechanism*		*Acid mechanisms*			*Base mechanism*		
Primary	*(cm^2/g)*	*k_{25} ($mol/m^2/s$)*	*E_a (kJ/mol)*	*k_{25} ($mol/m^2/s$)*	*E_a (kJ/mol)*	*$n(H^+)$*	*k_{25} ($mol/m^2/s$)*	*E_a (kJ/mol)*	*$n(H^+)$*
Ca,Al Pyroxene[a,b,c]	2								
Diopside[a,c]	2	7.943×10^{-15}	40.6	4.365×10^{-15}	96.1	0.710			
Hedenbergite[a,b,c]	2								
Ferrosilite[a,b,c]	2								
Enstatite[a,c]	2	1.906×10^{-16}	80.0	9.550×10^{-13}	80.1	0.710			
Albite[a,c]	2	1.377×10^{-15}	69.8	3.459×10^{-13}	65.0	0.457	1.256×10^{-18}	71.0	-0.572
K-Feldspar[a,c]	2	1.945×10^{-15}	38.0	4.355×10^{-13}	51.7	0.500	3.155×10^{-24}	94.1	-0.823
Secondary									
Calcite[d]									
Hematite[a]	100	2.519×10^{-15}	66.2	2.570×10^{-09}	66.2	1.000			
Magnetite[a]	2	1.660×10^{-11}	18.6	2.570×10^{-09}	18.6	0.279			
Chamosite[e]	2	3.020×10^{-13}	88.0	7.762×10^{-13}	88.0	0.500			
Clinochlore[e]	2								
Quartz[f]	2	1.223×10^{-12}	80.5						
Epidote[a]	2	1.020×10^{-12}	70.7	2.510×10^{-11}	71.1	0.338	4.680×10^{-18}	79.1	-0.556
Potential alteration mineral									
Secondary									
Ankerite[g]	100	1.260×10^{-09}	62.8	6.457×10^{-04}	36.1	0.500			
Magnesite[a]	100	4.571×10^{-10}	23.5	4.169×10^{-07}	14.4	1.000			
Siderite[h]	100	1.260×10^{-09}	62.8	1.590×10^{-04}	45.0	0.900			
Anhydrite[d]									
Pyrite[a]	100	2.000×10^{-10}	50.8	3.020×10^{-08}	50.8	-0.500 $n(FE^{+3}) = 0.500$	2.818×10^{-05}	56.9	0.500[i]
Pyrrhotite[a]	100	2.000×10^{-10}	50.8	3.020×10^{-08}	50.8	0.597			
Saponite-Fe-Fe[j]	100								
Saponite-Fe-K[j]	100								
Saponite-Mg-Mg[j]	100	1.659×10^{-13}	35.0	1.047×10^{-13}	23.6	0.340	3.020×10^{-17}	58.9	-0.400
Saponite-Mg-K[j]	100								
Saponite-Mg-Fe[j]	100								
Montmorillonite-Ca[k]	100								
Montmorillonite-K[k]	100	3.890×10^{-15}	48.0	1.950×10^{-13}	48.0	0.220	3.898×10^{-12}	78.0	-0.130
Montmorillonite-Mg[k]	100								
Montmorillonite-Na[k]	100								
Analcime[l]	100								
Laumontite[l]	100								
Mordenite-Ca[l]	100	1.590×10^{-12}	58.0	2.000×10^{-08}	58.0	0.700	5.50×10^{-15}	58.0	-0.300
Stilbite-Ca[l]	100								
Thomsonite[l]	100								
Wairakite[l]	100								
$SiO_{2\ (am)}$[m]	100	7.320×10^{-13}	60.9						
Prehnite[a]	100	6.920×10^{-14}	93.4	2.190×10^{-11}	80.5	0.256	1.380×10^{-15}	93.3	-0.200
Wollastonite[a]	100	1.585×10^{-09}	54.7	7.244×10^{-08}	50.8	1.000			
Kaolinite[a]	100	6.607×10^{-14}	22.2	4.898×10^{-12}	22.2	0.777	8.912×10^{-18}	17.9	0.472

[a] From Palandri and Kharaka (2004).
[b] Ca,Al Pyroxene, Hedenbergite and Ferrosilite are assumed to have the same rate law as Diopside.
[c] Rate constants reduced by 3 orders of magnitude.
[d] Under equilibrium constraint.
[e] Chlorites assumed to have the same rate law as Clinochlore 14 Å from Palandri and Kharaka (2004).
[f] From Gíslason et al. (1997).
[g] Kinetic parameters for Ankerite are set to those of Siderite.
[h] From Knauss et al. (2005).
[i] Reaction order n with respect to O2.
[j] Based on smectite ($K_{0.04}Ca_{0.5}(Al_{2.8}Fe_{0.53}Mg_{0.7})(Si_{7.65}Al_{0.35})O_{20}(OH)_4$) from Palandri and Kharaka (2004).
[k] Based on Montmorillonite, ($K_{0.318}(Si3_{.975}Al_{0.025})(Al_{1.509}Fe_{0.205}Mg_{0.283})(OH)_2$) from Palandri and Kharaka (2004).
[l] All zeolites assumed to have the same rate law as heulandite.
[m] From Rimstidt and Barnes (1980). Precipitation occurs under the free energy rate law of Carroll et al. (1998).
[n] Kinetic parameters for Ferroactinolite are set to those of Tremolite.